OPEN

Paper

Patient-specific Extravasation Dosimetry Using Uptake Probe Measurements

Dustin Osborne,[1] Jackson W. Kiser,[2] Josh Knowland,[3] David Townsend,[4] and Darrell R. Fisher[5]

Abstract—**Extravasation is a common problem in radiopharmaceutical administration and can result in significant radiation dose to underlying tissue and skin. The resulting radiation effects are rarely studied and should be more fully evaluated to guide patient care and meet regulatory obligations. The purpose of this work was to show that a dedicated radiopharmaceutical injection monitoring system can help clinicians characterize extravasations for calculating tissue and skin doses. We employed a commercially available radiopharmaceutical injection monitoring system to identify suspected extravasation of ^{18}F-fluorodeoxyglucose and ^{99m}Tc-methylene diphosphonate in 26 patients and to characterize their rates of biological clearance. We calculated the self-dose to infiltrated tissue using Monte Carlo simulation and standard MIRD dosimetry methods, and we used VARSKIN software to calculate the shallow dose equivalent to the epithelial basal-cell layer of overlying skin. For 26 patients, injection-site count rate data were used to characterize extravasation clearance. For each, the absorbed dose was calculated using representative tissue geometries. Resulting tissue-absorbed doses ranged from 0.6 to 11.2 Gy, and the shallow dose equivalent to a 10 cm^2 area of adjacent skin in these patients ranged from about 0.1 to 5.4 Sv. Extravasated injections of radiopharmaceuticals can result in unintentional doses that exceed well-established radiation protection and regulatory limits; they should be identified and characterized. An external injection monitoring system may help to promptly identify and characterize extravasations and improve dosimetry calculations. Patient-specific characterization can help clinicians determine extravasation severity and whether the patient should be followed for adverse tissue reactions that may present later in time.**
Health Phys. 120(3):339–343; 2021

Key words: extravasation; internal dosimetry; radiation dose; biokinetics; extremity dose

INTRODUCTION

Most diagnostic nuclear medicine exams and therapeutic infusions are accomplished by administering radiopharmaceuticals intravenously (Boellaard et al. 2015). An extravasation, also known as an infiltration, occurs when a radiopharmaceutical is inadvertently injected into tissue surrounding the injection site instead of into the vasculature. Extravasations can result from improper initial placement of the intravenous (IV) access device or by failure of the vessel wall (Hadaway 2007). Extravasations occur relatively frequently (mean 10.4%, N = 5418, 20 nuclear medicine centers), as previously described (Hall et al. 2006; Bains et al. 2009; Krumrey et al. 2009; Osman et al. 2011; Silva-Rodriguez et al. 2014; McIntosh and Abele 2016; Muzaffar et al. 2017; Wong et al. 2019; Currie and Sanchez 2020) and can result in significant dose to underlying tissues and skin (Patton and Millar 1950; Shapiro et al. 1987; Rhymer et al. 2010; Bonta et al. 2011; Kawabe et al. 2013; Goodman and Smith 2015; van der Pol et al. 2017; Tylski et al. 2018). However, because radiation effects on patients may take years to manifest and are rarely studied (van der Pol et al. 2017), dose resulting from extravasations should be more fully evaluated.

Factors that influence tissue absorbed dose from extravasation include infiltrated tissue volume as well as radioactivity distribution, retention, absorption, and clearance. Extravasation clearance rate has been estimated to be 2 to 10 h (Esser 2017). Serial imaging with positron emission tomography (PET) or single-photon-emission computed tomography (SPECT) can provide more accurate estimates of radioactivity and clearance (Breen and Dreidger 1991; Williams et al. 2006; Bonta et al. 2011; Terwinghe et al. 2012; Kawabe et al. 2013; Tylski et al. 2018). However, clinicians must promptly recognize that a tissue infiltration has occurred, imaging systems must be available, and staff must know how to evaluate the resulting extravasation image data. In lieu of

[1]University of Tennessee Graduate School of Medicine, Knoxville TN; [2]Carilion Clinic, Roanoke, VA; [3]Lucerno Dynamics LLC, Cary NC; [4]Independent Scholar; [5]Washington State University and Versant Medical Physics and Radiation Safety, Richland, WA.

For correspondence contact Josh Knowland, 140 Towerview Court, Cary, NC 27513, or email at **jknowland@lucernodynamics.com**.

(*Manuscript accepted* 23 *September* 2020)

0017-9078/21/0

DOI: 10.1097/HP.0000000000001375

imaging, manual serial measurements of the injection site can be made using a scintillation counter or other radiation detection system to determine retention and clearance parameters (Esser 2017). This manuscript describes an efficient, automated serial measurement system used to identify and characterize radiopharmaceutical extravasations.

Radiation dose estimates guide decision-making with respect to follow-up actions that may be appropriate. The purpose of this work was to show that a dedicated radiopharmaceutical injection monitoring system can help clinicians and technologists characterize extravasations for calculating tissue and skin doses.

MATERIALS AND METHODS

Radiation detector

We employed a commercially available detector (Lara® System, Lucerno Dynamics, Cary, NC) to characterize 26 extravasations of ^{18}F-fluorodeoxyglucose (^{18}F-FDG) and ^{99m}Tc-methylene diphosphonate (^{99m}TC-MDP). The Lara radiopharmaceutical injection monitoring system comprises one scintillation detector placed on the patient's skin proximal to the injection site and another on the opposite arm as a reference (Fig. 1). Each detector incorporates a single bismuth germanate (BGO) crystal and a silicon photomultiplier (SiPM). The detectors are neither shielded nor collimated, so their response is omnidirectional. Photon energy response is variable, depending on radionuclide, as previously described (Knowland et al. 2018). Each Lara detector records photon counts per second (cps) and generates a plot of counts vs. time. Reference detector output may be subtracted from injection-site detector output to correct for background photon counts such as from photons originating in the patient's torso.

Radiation dosimetry

Using mathematical methods (Bolch et al. 2009) recommended by the special committee on Medical Internal Radiation Dose (MIRD) of the Society of Nuclear Medicine and Molecular Imaging (SNMMI), we calculated radiation absorbed doses (Gy) to representative volumes (cm^3) of subdermal tissue containing infiltrated radiopharmaceutical.

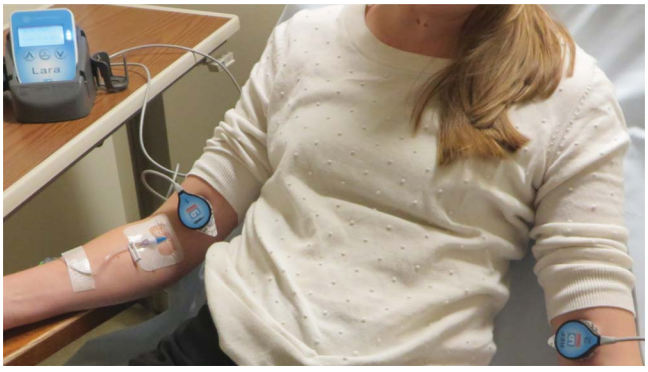

Fig. 1. Photo of the injection monitoring system used on a nuclear medicine patient.

Using a slightly modified version of VARSKIN 6.1 (Hamby and Mangini 2018), a computer code for skin dosimetry, we also calculated the shallow dose equivalent (Sv) to the highest relevant area of the skin (10 cm^2).

In the MIRD formalism, the absorbed dose $D(r_T \leftarrow r_S)$ from activity in a source region that irradiates a target region is $D(r_T \leftarrow r_S) = \tilde{A}(r_S, \tau)\ \Sigma_i\ \Delta_i\ \varphi_i(r_T \leftarrow r_S)/m_T$, where $\tilde{A}(r_S, \tau)$ is the time-integrated activity in the source region, and $\tilde{A}(r_S, \tau) = \int_0^{\tau} A(r_S, t)dt$, where Δ_i is the mean energy emitted per decay or transformation, where $\varphi_i(r_T \leftarrow r_S)$ is the absorbed fraction (fraction of energy emitted from a source region that deposits in a target region), and where m_T is the mass of the target region (Bolch et al. 2009). When calculating absorbed dose to infiltrated tissue, the source and target regions are the same ($r_T = r_S$); that is, the self-dose to infiltrated tissue.

Count-rate curve

To determine the time-dependent number of radioactive decays in the source region from an extravasation, we used the Lara detector count-rate curve (one measurement per second), which reflects the "effective" disappearance of infiltrated activity (combined effects of radioactive decay and biological clearance) following 26 extravasations of ^{18}F-FDG or ^{99m}Tc-MDP. We then identified an appropriate mathematical function for the curve and best-fit parameters by least-squares regression analysis using commercially available curve-fitting software (Curve Expert Professional, Hyams Developent, Huntsville, AL). We integrated analytically to yield area under the fitted curve representing total counts from injection through complete disappearance.

Converting counts to activity present

Detector photon count rate can be converted to absolute activity (MBq) using a three-dimensional region of interest (ROI) within the patient's nuclear medicine image. We determined an activity calibration factor by dividing the fitted curve at imaging time by the ROI activity. We then converted the fitted curve to units of activity by multiplying it by the calibration factor. In the absence of quantifiable injection-site image data (e.g., injection site outside of the imaging field-of-view), extravasated activity was estimated based on overall image quality relative to a non-extravasated infusion.

Absorbed energy fraction

In the MIRD schema, the absorbed fraction $\varphi_i(r_T \leftarrow r_S)$ can be determined experimentally using calibration sources and phantoms, or it may be calculated using Monte Carlo track simulations. Infiltrated tissue may present in many different shapes and sizes. To assess and compare potential tissue doses, we used Monte Carlo simulations and modeled the infiltrated tissue as one of three representative geometries of unit-density tissue: (a) a thin, right circular cylinder having a radius (r, cm) and height (h, cm) lying beneath the dermis where the tissue volume = π r^2 h (cm^3), (b) as a sphere

where the tissue volume = $(4\ \pi\ r^3)/3$, and (c) as an ellipsoid where the tissue volume = $(4\ \pi\ a\ b\ c)/3$ where a, b, and c were the radii of the ellipsoid. We calculated absorbed fractions for each representative geometry using the GEANT4 Application for Tomographic Emission (GATE)[6] Monte Carlo simulation code. Each simulation consisted of 1 MBq distributed uniformly within water.

Subdermal tissue self-dose

The mass of infiltrated tissue depends on the volume of extravasated radiopharmaceutical and penetration into the subdermal fascia. We calculated the absorbed doses (Gy) to infiltrated tissues by taking into account the tissue mass, total energy emitted in the source region, and the energy absorbed fraction according to the MIRD schema (Bolch et al. 2009).

Relevant skin dose

The National Council on Radiation Protection and Measurements recommends (NCRP 2018) for occupational exposure that the absorbed dose in skin at a depth of 70 μm be limited to 0.5 Gy averaged over the most highly exposed 10 cm^2 of skin. Skin dose assessments in units of shallow dose equivalent (Sv) are required by the Code of Federal Regulations in 10 CFR 20.1201(c) for a contiguous 10 cm^2 area of skin at a tissue depth of 0.007 cm (7 mg cm^{-2}). For regulatory compliance with recommended skin dose limits, the software code VARSKIN, version 6.1 (Hamby and Mangini 2018), was written to calculate occupational dose from radioactive contamination on or near the skin. We applied it to patient radiopharmaceutical infiltrations. For cases involving low-LET radiations, dose expressed in units of Gy and Sv are numerically (approximately) equivalent.

Because infiltrated tissue lies beneath and adjacent to the skin epidermis, we defined the relevant target for calculating dose to overlying skin as a thin layer comprising the sensitive epithelial basal cells with an area of 10 cm^2 and at a tissue depth beneath the skin surface of 0.007 cm (70 μm or 7 mg cm^{-2}). We assumed that the dose limits to patient skin should be the same or less than those for occupational exposures. We modeled infiltrated subdermal tissue as a three-dimensional thin cylinder, and calculated the relevant skin dose using a modified VARSKIN 6.1 computer code by setting the distance between the infiltrated source tissue and the sensitive basal cell layer to 10 μm (1 mg cm^{-2}) and removing backscatter correction.

RESULTS

Fig. 2 shows one example of the 26 actual recorded count rate data and the corresponding curve fit to a single-exponential function for an extravasated patient.

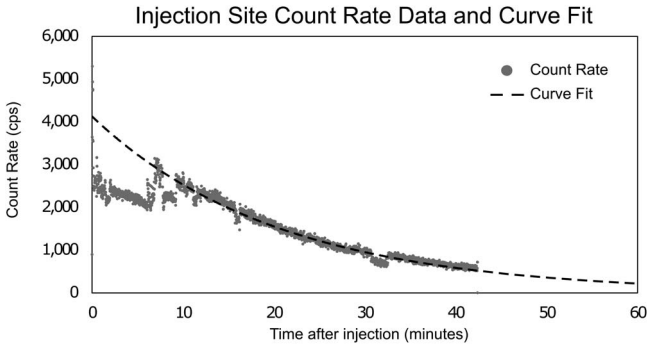

Fig. 2. Injection site count rate data with fitted curve for one example case.

Details of the tissue geometries modeled for each infiltration, together with calculated energy absorbed fractions for ^{18}F and ^{99m}Tc are shown in Table 1. Infiltrated tissue self-dose (Gy) and the skin shallow dose equivalent (Sv) for 26 infiltrated patients are show in Table 2. In each case, either (or both) the infiltrated tissue dose or the adjacent skin shallow dose equivalent exceeded the limiting value 0.5 Gy or 0.5 Sv.

DISCUSSION

In this work, we investigated extravasations of ^{18}F-FDG and ^{99m}Tc-MDP, but the methods described herein also apply to all other radiopharmaceuticals and amounts administered. The positron energy of ^{18}F resulted in significant tissue self-dose and significant dose to overlaying skin. Despite the relatively low absorbed fractions for ^{99m}Tc, we found that ^{99m}Tc-labeled agents can produce significant tissue absorbed doses. Our results in 26 cases exceeded radiation protection (NCRP 2018) and regulatory[7] limits for extremity tissue (0.5 Gy) and skin (0.5 Sv).

The literature contains several examples of adverse tissue reactions following extravasation of diagnostic and therapeutic radioisotopes such as ^{201}Tl (van der Pol et al. 2017), ^{90}Y (Williams et al. 2006; Siebeneck 2008), ^{89}Sr (Kawabe et al. 2013), ^{131}I (Breen and Dreidger 1991; Bonta et al. 2011; van der Pol et al. 2017), and ^{32}P (Minsky et al. 1987). We found one published example of radiopharmaceutical extravasation leading directly to a highly localized cancerous lesion (Benjegerdes et al. 2017): following extravasation of ^{223}Ra-dichloride, the patient developed aggressive squamous cell carcinoma at the injection site.

Because extravasations are common (Wong et al. 2019) and can lead to adverse tissue reaction, prompt identification and mitigation are important factors. In our review, none of the technologists or patients reported immediate

[6] OpenGATE Collaboration. Available at http://www.opengatecollaboration.org/. Accessed 25 August 2020.

[7] 10CFR Part 35, Medical use of byproduct material. Available at https://www.nrc.gov/reading-rm/doc-collections/cfr/part035/. Accessed 25 August 2020.

Table 1. Representative tissue geometry details and energy absorbed fractions.

Geometry	Dimensions (cm)	Absorbed fraction for ^{18}F	Absorbed fraction for ^{99m}Tc
Cylinder	h = 0.1, r = 4	73%	11%
Ellipsoid	a = 2.13, b = 1.07, c = 0.53	95%	13%
Sphere	r = 1.07	97%	13%

pain or edema during or following the injection—even in cases of extravasation—emphasizing the difficulty in prompt extravasation identification. Mitigation steps such as elevation of the arm, application of heat (Yucha et al. 1994; Goolsby and Lombardo 2006), and flushing with saline can accelerate clearance and decrease radiation doses.

Once an extravasation has been identified, accurate dose calculation enables clinicians to identify patients who should be followed for adverse tissue reactions or late stochastic effects. Absence of immediate visible skin reactions is a common explanation for not reporting and following up after extravasation events.[8] However, given the expected time for presentation of symptoms, it is unlikely that extravasation-related injury would be discovered. van der Pol et al. (2017) reported that, despite an extensive literature review, only 3,016 published cases of diagnostic radiopharmaceutical extravasation were found. Of those, only three cases included dosimetry calculation and patient follow-up. All three patients who were followed were found to suffer adverse tissue reactions. In one case, a radiation ulcus was diagnosed after 2 y. In a second case, the radiation ulcus diagnosis was made after 3 y. Of the remaining 3,013 cases, none described dosimetric parameters or follow-up (van der Pol et al. 2017).

In cases of ^{99m}Tc-MDP extravasation, immediate skin reactions are not likely. Our data review suggests that the shallow dose equivalent to the skin may be low even in cases where the absorbed dose to infiltrated tissue is high. Absence of prompt skin reactions should not dissuade clinicians from considering delayed detrimental effects to tissue and skin. Proper documentation and patient follow-up may protect medical institutions from frivolous litigation and unwarranted regulatory review.

CONCLUSION

Extravasation events in nuclear medicine are rarely fully characterized—including accurate dosimetry and appropriate clinical follow-up. Accurate dosimetry should include the determination of infiltrated fraction of administered activity, clearance half-times, and resulting radiation doses to infiltrated tissue and overlaying skin. We investigated injection-site count-rate data for 26 cases of extravasation of ^{18}F-FDG and ^{99m}Tc-MDP, assuming three source-tissue geometries. For cases reported in this paper, radiation absorbed doses to infiltrated tissue ranged from 0.6 Gy to 11.2 Gy, and the shallow dose equivalent to a 10 cm^2 area of adjacent skin ranged from about 0.1 Sv to 5.4 Sv.

Table 2. Detailed dosimetry results.

Case #	Radiopharmaceutical	Effective clearance half-time (min)	Mean absorbed dose to infiltrated fascia (Gy)	Shallow dose equivalent to skin (Sv)
1	^{18}F-FDG	9	0.6	0.3
2	^{18}F-FDG	43	7.6	3.7
3	^{18}F-FDG	93	2.7	1.3
4	^{18}F-FDG	24	8.4	4.1
5	^{18}F-FDG	13	0.8	0.4
6	^{18}F-FDG	22	0.7	0.3
7	^{18}F-FDG	44	0.9	0.4
8	^{18}F-FDG	39	11.2	5.4
9	^{18}F-FDG	70	1.0	0.5
10	^{18}F-FDG	38	8.7	4.2
11	^{18}F-FDG	22	3.8	1.9
12	^{18}F-FDG	41	0.6	0.3
13	^{99m}Tc-MDP	360	8.4	< 0.1
14	^{18}F-FDG	46	1.0	0.5
15	^{99m}Tc-MDP	64	1.5	< 0.1
16	^{99m}Tc-MDP	218	5.3	< 0.1
17	^{99m}Tc-MDP	38	0.9	< 0.1
18	^{99m}Tc-MDP	49	1.2	< 0.1
19	^{99m}Tc-MDP	64	1.5	< 0.1
20	^{18}F-FDG	18	1.1	0.5
21	^{18}F-FDG	22	5.1	2.5
22	^{99m}Tc-MDP	36	0.9	< 0.1
23	^{18}F-FDG	24	6.8	3.3
24	^{18}F-FDG	79	2.9	1.4
25	^{18}F-FDG	26	0.8	0.4
26	^{18}F-FDG	22	3.6	1.8

With patient radiation safety in mind, we maintain that both diagnostic and therapeutic extravasation events should be identified and characterized. Severe extravasations affect the diagnostic or therapeutic quality of nuclear medicine procedures, and the unintended dose to tissue and skin may eventually be clinically significant. A dedicated radiopharmaceutical injection monitoring system can be used to improve the accuracy of dosimetry and assist in determining the need for patient follow-up.

Acknowledgments—The authors are thankful for the generous assistance provided by Augusto Giussani of the Department of Medical and Occupational Radiation Protection within the German Federal Office for Radiation Protection. We also thank David Hamby, Oregon State University, Corvallis, for

[8]Official Transcript of Proceedings, NRC ACMUI. Available at https://www.nrc.gov/docs/ML0903/ML090340745.pdf. Accessed 25 August 2020

helpful advice concerning modification and implementation of VARSKIN 6.1 for deep-tissue sources.

Dustin Osborne is conducting research with Lucerno Dynamics unrelated to this manuscript and received no financial compensation for this work. Jackson W Kiser provides consultancy services for Lucerno Dynamics but received no financial compensation for this work. Josh Knowland is an employee of Lucerno Dynamics, the manufacturer of the Lara System. David Townsend has no competing interests to disclose. Versant Medical Physics and Radiation Safety (Kalamazoo, Michigan) provides consultant services to Lucerno Dynamics, but did not contribute to or receive payment for this work.

REFERENCES

Bains A, Botkin C, Oliver D, Nguyen N, Osman M. Contamination in ^{18}F-FDG PET/CT: an initial experience. J Nucl Med 50(Suppl 2):2222; 2009.

Benjegerdes KE, Brown SC, Housewright CD. Focal cutaneous squamous cell carcinoma following radium-223 extravasation. Proc Bayl Univ Med Cent 30:78–79; 2017.

Boellaard R, Delgado-Bolton R, Oyen WJG, Giammarile F, Tatsch K, Eschner W, Verzijlbergen FJ, Barrington SF, Pike LC, Weber WA, Stroobants S, Delbeke D, Donohoe KJ, Holbrook S, Graham MM, Testanera G, Hoekstra OS, Zijlstra J, Visser E, Hoekstra CJ, Pruim J, Willemsen A, Arends B, Kotzerke J, Bockisch A, Beyer T, Chiti A, Krause BJ. FDG PET/CT: EANM procedure guidelines for tumour imaging: version 2.0. Eur J Nucl Med Mol Imaging 42:328–354; 2015.

Bolch WE, Eckerman KF, Sgouros G, Thomas SR. MIRD pamphlet No. 21: A generalized schema for radiopharmaceutical dosimetry—standardization of nomenclature. J Nuc Med 50(3): 477–484; 2009.

Bonta DV, Halkar RK, Alazraki N. Extravasation of a therapeutic dose of ^{131}I-metaiodobenzylguanidine: prevention, dosimetry, and mitigation. J Nucl Med 52:1418–1422; 2011.

Breen SL, Dreidger AA. Radiation injury from interstitial injection of iodine-131-iodocholesterol. J Nucl Med 32:892; 1991.

Esser JB (ed). Procedure guidelines nuclear medicine. Dutch Society of Nuclear Medicine (NVNG), 2nd ed. rev. (English). Neer, Netherlands:HGP Vullers/Kloosterhof Neer BV. ISBN 978-90-78876-09-0. Undated.

Goodman S, Smith J. Patient specific dosimetry of extravasation of radiopharmaceuticals using Monte Carlo (abstract). Proc Royal Australian College of Physicians. Intern Med J 45(Suppl 1): 1; 2015.

Goolsby TV, Lombardo FA. Extravasation of chemotherapeutic agents: prevention and treatment. Semin Oncol 33:139–143; 2006.

Hadaway L. Infiltration and extravasation. Am J Nurs 107:64–72; 2007.

Hall N, Zhang J, Reid R, Hurley D, Knopp M. Impact of FDG extravasation on SUV measurements in clinical PET/CT. Should we routinely scan the injection site? J Nucl Med 47(Suppl 1): 115P; 2006.

Hamby DM, Mangini CD. VASKIN 6: a computer code for contamination dosimetry. Rockville, MD: NRC; NUREG-CR-6918; 2018.

Kawabe J, Higashiyama S, Kotani K, Yoshida A, Tsushima H, Yamanaga T, Tsuruta D, Shiomi S. Subcutaneous extravasation of Sr-89: Usefulness of Bremsstrahlung Imaging in confirming Sr-89 extravasation and in the decision making for the choice of treatment strategies for local radiation injuries caused by Sr-89 extravasation. Asia Ocean J Nucl Med Biol 1:56–59; 2013.

Knowland J, Lipman S, Lattanze RK, Kingg JB, Ryan KA, Perrin SR. Characterization of technology to detect injection site radioactivity. J Med Phys 46(6):2690–2695; 2019.

Krumrey S, Frye R, Tran I, Yost P, Nguyen N, Osman M. FDG manual injection verses infusion system: a comparison of dose precision and extravasation. J Nucl Med 50(Suppl 2): 2031; 2009.

McIntosh C, Abele J. Frequency of interstitial radiotracer injection for patients undergoing bone scan. Montreal, Quebec: The Canadian Association of Radiologists; 2016.

Minsky BD, Siddon RL, Recht A, Nagel JS. Dosimetry of aqueous ^{32}P after soft-tissue infiltration following attempted intravenous administration. Health Phys 52:87–89; 1987.

Muzaffar R, Frye SA, McMunn A, Ryan K, Lattanze R, Osman MM. Novel method to detect and characterize (18)F-FDG infiltration at the injection site: a single-institution experience. J Nucl Med Technol 45:267–271; 2017.

National Council on Radiation Protection and Measurements. Management of exposure to ionizing radiation: Radiation Protection Guidance for the United States. Bethesda, MD: NCRP; NCRP Report No. 180; 2018.

Osman MM, Muzaffar R, Altinyay ME, Teymouri C. FDG dose extravasations in PET/CT: frequency and impact on SUV measurements. Front Oncol 1:41; 2011. Available online at: https://doi.org/10.3389/fonc.2011.00041.

Patton HS, Millar RG. Accidental skin ulcerations from radioisotopes: recognition, prevention and treatment. J Am Med Assoc 143:554–555; 1950.

Rhymer SM, Parker JA, Palmer MR. Detection of ^{90}Y extravasation by Bremsstrahlung imaging for patients undergoing ^{90}Y-ibritumomab tiuxetan therapy. J Nucl Med Technol 38: 195–198; 2010.

Sanchez S, Currie GM. Topical sensor for the assessment of injection quality for ^{18}F-FDG, ^{68}Ga-PSMA and ^{68}Ga-DOTATATE positron emission tomography. J Med Imag Radiat Sci 51(2): 247–255; 2020.

Shapiro B, Pillay M, Cox PH. Dosimetric consequences of interstitial extravasation following i.v. administration of a radiopharmaceutical. Eur J Nucl Med 12:522–523; 1987.

Siebeneck BM. Extravasation of yttrium-90 ibritumomab tiuxetan: a case study. Clin J Oncol Nurs 12:275–278; 2008.

Silva-Rodriguez J, Aguiar P, Sanchez M, Mosquera J, Luna-Vega V, Cortes J, Garrido M, Pombar M, Ruibal A. Correction for FDG PET dose extravasations: Monte Carlo validation and quantitative evaluation of patient studies. Med Phys 41:052502; 2014.

Terwinghe C, Binnebeek SV, Bergans N, Haustermans K, Van Custem E, Verbruggen A, Deroose CM, Vanbilloen B, Baeste K, Koole M, Verslype C, Clement PM, Mortelmans L. Extravasation of Y-DOTATOC: case report and discussion of potential effects, remedies and precautions in PRRT. Eur J Nucl Med Mol Imaging 39(S205):155–303; 2012.

Tylski P, Vuillod A, Goutain-Majorel C, Jalade P. Abstract 58, dose estimation for an extravasation in a patient treated with ^{177}Lu-DOTATATE. Physica Medica 56:32–33; 2018.

van der Pol J, Voo S, Bucerius J, Mottaghy FM. Consequences of radiopharmaceutical extravasation and therapeutic interventions: a systematic review. Eur J Nucl Med Mol Imaging 44: 1234–1243; 2017.

Williams G, Palmer MR, Parker JA, Joyce R. Extravazation of therapeutic yttrium-90-ibritumomab tiuxetan (zevalin): a case report. Cancer Biother Radiopharm 21:101–105; 2006.

Wong TZ, Benefield T, Masters S, Kiser JW, Crowley JR, Osborne D, Mawlawi O, Barnwell J, Gupta P, Mintz A, Ryan K, Perrin SR, Lattanze RK, Townsend DW. Quality improvement initiatives to assess and improve PET/CT injection infiltration rates in multiple centers. J Nucl Med Technol 47:326–331; 2019.

Yucha CB, Hastings-Tolsma M, Szeverenyi NM. Effect of elevation on intravenous extravasations. J Intraven Nurs 17: 231–234; 1994.